Taylor & Francis
Taylor & Francis Group

Journal of Microwave Power and Electromagnetic Energy

ISSN: 0832-7823 (Print) (Online) Journal homepage: https://www.tandfonline.com/loi/tpee20

Effects of power input and food aspect ratio on microwave thawing process of frozen food in commercial oven

Waraporn Klinbun & Phadungsak Rattanadecho

To cite this article: Waraporn Klinbun & Phadungsak Rattanadecho (2019): Effects of power input and food aspect ratio on microwave thawing process of frozen food in commercial oven, Journal of Microwave Power and Electromagnetic Energy, DOI: 10.1080/08327823.2019.1677430

To link to this article: https://doi.org/10.1080/08327823.2019.1677430

Published online: 09 Nov 2019.

JOURNAL OF MICROWAVE POWER AND ELECTROMAGNETIC ENERGY
https://doi.org/10.1080/08327823.2019.1677430

Effects of power input and food aspect ratio on microwave thawing process of frozen food in commercial oven

Waraporn Klinbun[a] and Phadungsak Rattanadecho[b]

[a]Department of Automotive Manufacturing Engineering, Faculty of Engineering and Technology, Panyapiwat Institute of Management, Pakkred, Nonthaburi, Thailand; [b]Department of Mechanical Engineering, Faculty of Engineering, Thammasat University (Rangsit Campus), Khlong Luang, Pathum Thani, Thailand

ABSTRACT

This research studied the effects of power level and aspect ratio by numerical and experimental analysis in the microwave heating process. The sample was congee frozen rice. A three-dimensional model developed to solve Maxwell's equations and Fourier's heat equations using the finite element method in COMSOL Multiphysics software. The simulated temperature results were validated experimental results to measure five locations temperature by fibre-optic sensors. The surface temperature was captured by an infrared camera. From the results, the RMSE values of transient temperature were between ranges of 6.14 and 12.88 °C. The calculated temperature contours were in a good agreement for the 300-s heating. In addition, the increasing heating rate was 27% at the higher power level (1300–1800 W). The aspect ratio of sample change was significant change uniformity occurred. Finally, the expected results from the study will provide a conceptual framework, critical parameters, and distribution of microwave oven applicable temperature for specific frozen food and its packing.

ARTICLE HISTORY
Received 10 January 2019
Accepted 15 June 2019

KEYWORDS
Food safety; non-uniform heating; numerical method; microwave heating; temperature distribution

1. Introduction

The ready-to-eat frozen food has been cooked and then rapidly frozen. The frozen storage was set lowering the product temperature generally to −18 °C or below. The frozen food examples were the dumpling, pizza, bread, potato puree, pasta, rice and vegetable soup. These foods were available in the market in many countries. However, the frozen foods have thawed before eating them. The most attractive thawing way was to use the microwave oven. That was convenient and easy. The microwave heating had many main advantages, such as fast accelerating rate due to volumetric heating, heating selectively, saving time and energy. However, a non-uniform electromagnetic wave field inside the oven cavity was a very concerning

CONTACT Waraporn Klinbun warapornkli@pim.ac.th

problem because it was leading to overheating and underheating region (or hot and cold spots) within the sample at the same time. Concerning microwave food safety issues, the non-uniform heating of food may cause burning of packaging or container. Thus, the effects of all parameters on the heating pattern within dielectric samples and electric field distribution inside the domestic oven were the key study of microwave heating processing.

There have been many types of research on thawing foods with microwave energy. The following researches were the example of related work. The effects of separation modes (vacuum-assisted and gravitational), temperatures of thawing (20, 4 and 1 °C), and mode of thawing (free thawing and microwave-assisted) on heat transfer of block freeze-concentration (FC) of coffee brews were studied (Moreno et al. 2013). From the results, microwave-assisted vacuum heating could improve the separation quality. Basak and Ayappa (2002) presented the 2D frozen cylinders which subjected to uniform plane waves from one side. The temperature-dependent effective specific heating capacity used in this model. For the one-dimensional model as noted by Delgado and Sun (2003), the objective of this work was to develop models of heat and mass transfer during thawing of cooked cured meat. A three-dimensional model of microwave heating developed for solving the coupled electromagnetic and heat transfer equation by Hoke et al. (2002), Pitchai et al. (2012), Llave et al. (2015), Llave et al. (2016), Punathil and Basak (2016), etc. Recently, the team of Koray Palazoğlu and Miran (2017) developed the model of microwave heating of frozen shrimp. The heating sources were microwave (915 MHz) and radiofrequency (27.12 MHz). A block of frozen shrimp (1.75 kg), heated from an initial temperature of −22 °C to between −5 and −3 °C. The simulation results agreed with experimental results. The results have shown that a uniform overall temperature distribution found for radiofrequency heating.

During microwave heating of frozen food, two key points were the magnitude of energy deposited inside dielectric materials and the uniformity of energy deposition inside the oven. First, it was oven features, such as size and shape of cavity and waveguide; mode stirrers and turntables (it could see in following works, such as Geedipalli et al. 2007; Pitchai et al. 2014; Chen et al. 2016; Meng et al. 2018); power and frequency of EM (it could see in following works, such as Taher and Farid 2001; Fouad 2013; He et al. 2014; Chen et al. 2016; Liu et al. 2017) and feed location (it could see in the work of Boillereaux et al. 2013). Second, it was food properties, such as size and shape of food (it could see in following works, such as Basak 2003; Rattanadecho 2004; Lee and Marchant 2004; Rakesh and Datta 2013); dielectric and thermal properties (it could see in following works, such as Guttman et al. 1980; Basak and Ayappa 1997; Erchiqui et al. 2015; Llave et al. 2016). The frozen food may be assumed to be the solid object (it could see in following works such as Zhang and Datta 2003; Campañone et al. 2011; Punathil and Basak 2016) or porous medium (it could see in following works such as Rakesh and Datta 2013; Chen et al. 2014) in the model. Each assumed sample has a different heating pattern subjected to microwave energy. However, many of parameters still have not yet been investigated. A numerical study of frozen food was a complex model which needs to consider many complex terms and dramatic change in properties. Because of the frozen sample changed

phase during the microwave processing. The comprehensive model was computationally intensive which can help in guiding product formulation, developing cooking instruction, designing product layout, and packaging.

This work was (1) to develop a 3D model of microwave heating of Thai frozen food in the domestic oven, (2) to compare the simulated temperature to experiment results, and (3) to evaluate the effect of power level and aspect ratio of the sample on model prediction.

2. Materials

This work has presented heat and mass transport phenomena that occurred in ready to eat Thai frozen food during heating in the domestic oven. The impacts of power input levels and aspect ratio on electromagnetic field distribution inside the oven, the power absorption, and the temperature profile within the sample.

2.1. Sample handling and preparation

The sample was freezing congee with minced pork. The composition of foods included 85.20% congee, 12.30% of minced pork, and 2.5% of vegetable (dried Chinese mushroom, ginger, spring onion) by weight basis. The freezing congee with minced pork obtained from Thai frozen foods manufacturer. The sample in a microwaveable plastic container kept at −18 °C in a freezer until used for the experiment. The frozen sample size was a cylindrical slice 10 cm in diameter and 5 cm thick for electromagnetic wave thawing.

2.2. Properties analysis

2.2.1. Dielectric properties measurement

A portable dielectric measurement kit (Püschner GmbK & Co. KG, France) was an instrument to measure the complex permittivity of a sample. The dielectric probe was an open-ended coaxial resonator probe that microwave signals interact with the materials. When the frozen food was touching the probe, electromagnetic field fringed into the material under test and changed because of the dielectric properties of the sample. The reflected signal back to resonator has been determined and related to the dielectric properties by using the software. Finally, the measurement data are shown in graphical formats. The precision of the dielectric constant (ε') and loss factor (ε'') was less than 2% and 5%, respectively. The steps of measurement were following:

1. The instrument warmed up for 30 min.
2. The probe was calibrated using water at 25 °C.
3. The frozen food placed in a glass and dipped into a controlled temperature water bath.
4. The sample heated up from −18 to 80 °C and the dielectric properties collected for three times selected 10 °C intervals.

The infrared thermometer (Testo 845, German) captured surface temperature and inside temperature was measured using the thermocouple temperature sensor (Fluke 51 II, USA). The dielectric properties were obtained as a function of temperature and at 2.45 GHz at frozen and unfrozen stages. The overall error in the measurement should be about 5%. From Klinbun and Rattanadecho (2017), they reported dielectric properties of frozen Thai foods at the temperature range of −18 to 80 °C at 2.45 GHz. They found that the dielectric property values increased with the increasing temperature. This because sample composition changed during the heating process. These results indicated that dielectric properties significantly affected the heating rate and profile of frozen food during the microwave processing. From the work of Jiao et al. (2014), both dielectric constant and loss factor influenced the heating rate of food product in a radiofrequency heater. If the dielectric constant and loss factor were similarly valuing, the heating rate of the sample would reach a maximum point.

2.2.2. Thermal properties analysis

In this study, the thermal properties including thermal conductivity (k) and specific heat capacity (c_p) determined from mathematical models. The steps were following:

1. to obtain their nutritional values of frozen congee including protein, fat, carbohydrate, fibre, and ash by SGS (Thailand) Limited Laboratory Services.
2. to calculate the thermal properties of frozen congee components, such as density, specific heat, thermal conductivity by using the Choi and Okos equations (Choi 1986). The mathematical model developed for computing thermal properties of food components as functions of temperature in the range of −40 to 150 °C. The thermal properties of water and ice also developed.
3. to determine the thermal properties of frozen congee by using the parallel model given by Murakami and Okos (1989).

The density of the sample estimated from knowing density (ρ_i) and mass fraction (m_i) of the component using the formula:

$$\rho = \frac{1}{\sum_{i=1}^{n} \left({}^{m_i}/_{\rho_i} \right)} \tag{1}$$

where n was the number of components. The thermal conductivity of a food sample with including n components calculated from the weighted average of the thermal conductivity of the component (k_i).

$$k = \sum_{i=1}^{n} \nu_i k_i \tag{2}$$

where ν_i was the volume fraction of the component and calculated by:

$$\nu_i = \frac{\left(m_i/\rho_i\right)}{\sum_{i=1}^{n}\left(m_i/\rho_i\right)} \tag{3}$$

The specific heat of food material with n components can be estimated by:

$$c_p = \sum_{i=1}^{n}\left(m_i c_{pi}\right) \tag{4}$$

The ice and liquid water mix of frozen congee calculated at a temperature of −18 °C. The resulting thermal properties of the ice/water mix is then combined with the thermal properties of each remaining food constituent to determine the thermal properties of the food product. As noted, the ratio of ice and water was 50:50 at a temperature of 0 °C.

From the work of Klinbun and Rattanadecho (2017), the thermal properties related to dielectric constant and dielectric loss factor as a function of temperature.

2.3. Penetration depth, d_p

The depth of penetration was a measurement of how deep electromagnetic waves can penetrate inside a sample. On the other hand, it related to the amount of power absorption passed through the sample. The penetration depth was used to select the approximate thickness of food inside packages to ensure a relatively uniform microwave heating process.

From the equation of Buffler (1993):

$$d_p = \frac{\lambda_0\sqrt{2}}{2\pi}\left\{\varepsilon'\left[\sqrt{1+\left(\frac{\varepsilon''}{\varepsilon'}\right)^2}-1\right]\right\}^{-\frac{1}{2}} \tag{5}$$

where λ_0 was free space microwave wavelength (m) and equal to 0.122 m at 2.45 GHz.

The penetration depth of frozen congee was 33.58 cm at a frozen state (−18 to 0 °C) at 2.45 GHz. When congee defrosted, the penetration depth rapidly decreased (6.18 cm at 0 °C) because of the effect of frozen water of the sample. Frozen congee was contained at more than 80% moisture content as results in the measured properties dramatically changed with the proportion of water in food materials. The sample absorbed energy and changed phase in the range of temperature of −5 to −1 °C and the penetration depths reduced by about one-half when the temperature increased from −20 to 100 °C at frequencies from 300 to 3000 MHz (Chen et al. 2013).

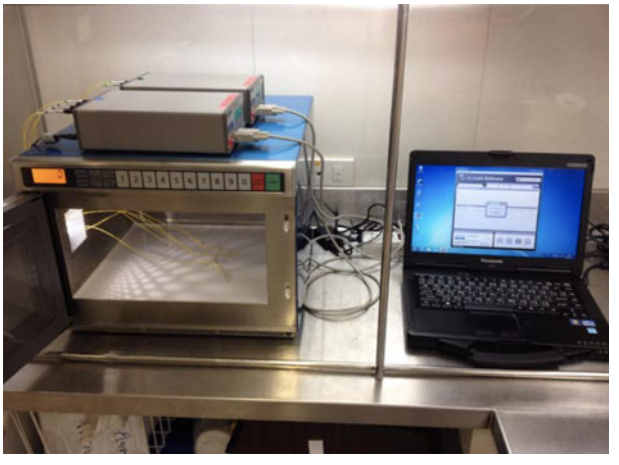

Figure 1. Experimental setup as microwave Panasonic NE1356 workstation.

3. Methods

3.1. Experimental thawing procedure

Figure 1 was the experimental setup in which the 7-Eleven microwave oven (Panasonic model No. NE1356) and fibre-optic thermometer (Luxtron, USA) were included. Experimental setup: (1) microwave control, (2) microwave cavity, (3) fibre-optic sensor, (4) data logger and (5) personal computer. The cavity dimension has a volume of 330 mm (width) × 310 mm (depth) × 175 mm (height) and an adjustable power output ranging from 340 W to 1300 W. The sample (frozen congee with minced pork) was placed on the plastic plate and located at the centre of the cavity throughout the experiments. In this study, the sample was heated at frequency of 2.45 GHz and heating duration of 300 s.

The microwave oven was 'ON' state. The magnetron generated the microwave and supplied it to the sample, thus, the sample's temperature increase was due to microwave heating. On the other hand, the magnetron did not generate microwave at 'OFF' state and this resulted in sample's temperature decrease was due to cooling by evaporation, convection and radiation. The resting time of the microwave oven was around 20 min for every experiment.

For the sample's temperature, the infrared imaging (IR-thermography) was used to capture temperature distribution on the top surface of the sample. Temperatures inside the sample were measured using a fibre-optic system during microwave heating. The temperature was registered five points during heating as seen in Figure 2. The fibre-optic system was connected to computers with a temperature logging system. The temperature data were sampled at 10-s interval using Luxtron TruTemp software. The experiment was repeated three times for increasing the accuracy and validity of the experimental data.

3.2. Computational method

To simulate the phenomena, first use Gauss law to obtain the electric field inside the microwave oven. Then, to solve heat conduction using Fourier's law with power

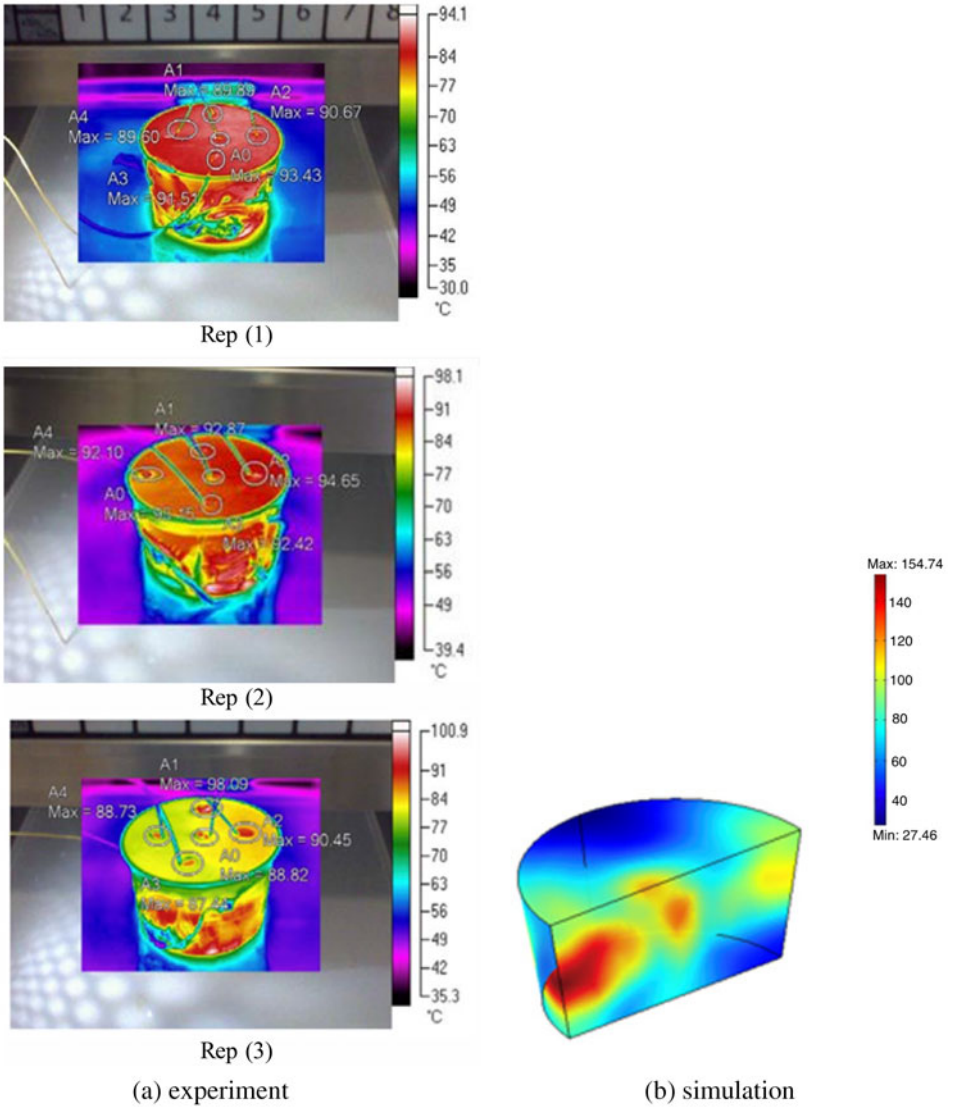

Figure 2. Simulation and average three replicates experimental time-temperature profile at three locations of congee subjected to 300 s heating in a 1300 W microwave oven.

generation required numerical computation. The distributed heat generation was computed in a stationary, frequency-domain electromagnetic analysis followed by a transient heat transfer simulation showing how the heat redistributed in the frozen congee.

3.2.1. Model geometry

Figure 3(b) shows the geometry of the model in software (COMSOL V. 4.3a, Comsol Inc., Boston, MA). The geometric model ($330 \times 310 \times 175$ mm) included a magnetron, a waveguide and a metal stirrer. The two ports that provided microwave energy to the cavity was located on top and bottom of the oven. The port was connected to a magnetron through a waveguide. The waveguide had cross-sectional dimensions of

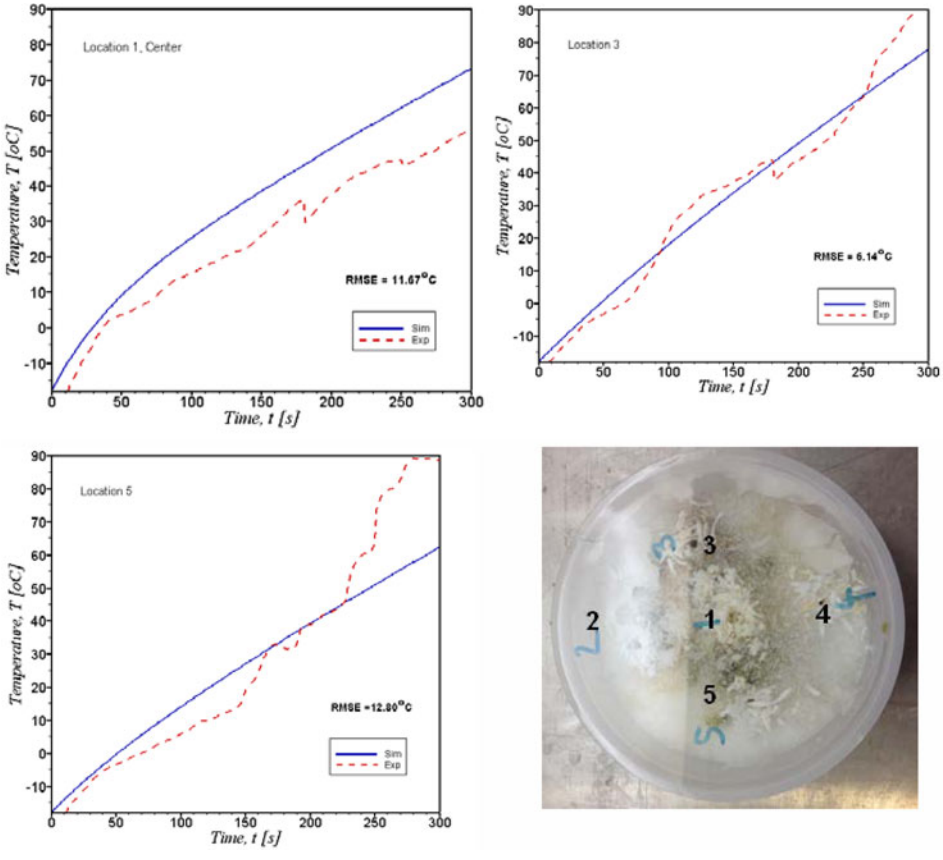

Figure 3. Comparison of temperature profiles after 300 s heating (P = 1300 W, f = 2.45 GHz).

86 mm (width) × 43 mm (height) and a length of 282 mm. The power source was a rectangular port feed with an operating frequency of 2.45 GHz.

Various microwave power levels (1300 W and 1800 W) and sample size (R04H06, R05H05, and R06H04) were investigated on the frozen congee. The microwave powers were selected because the powers were the highest power levels available in the 7-Eleven microwave oven. It was suggested that a high microwave power could provide an increasing accelerating thawing process.

3.2.2. Electromagnetic field equations

The Maxwell's equations were solved to obtain the 3D electric field distribution, $\vec{E}$, inside the microwave cavity and within the sample frozen food. There are following:

$$\nabla \times \mu_r^{-1}\left(\nabla \times \vec{E}\right) - \left(\frac{2\pi f}{c}\right)^2 (\varepsilon' - i\varepsilon')\,\vec{E} = 0 \tag{6}$$

where f was the microwave frequency (Hz), c was a speed of light (ms^{-1}), $\varepsilon', \varepsilon'', \mu_r$ were the dielectric constant, dielectric loss factor and relative permeability, respectively.

The electromagnetic wave penetrated into the sample and converted into thermal energy. The microwave power absorbed in the food material was proportional to the dielectric factor (ε'') and square of the electric field strength $\left(\left|\vec{E}\right|^2\right)$. Conversion of electromagnetic energy into thermal energy was governed by the following equation.

$$Q_{\text{abs}} = 2\pi f \cdot \varepsilon_0 \cdot \varepsilon'' \cdot \left|\vec{E}\right|^2 \tag{7}$$

where Q_{abs} was the dissipated power per unit volume [W m^{-3}] and ε_0 was the permittivity of the free space (8.854×10^{-12} Fm^{-1}).

The boundary conditions of metallic waveguide walls were considered as perfect electric conductors (PEC). The following boundary condition applied:

$$E_{\text{tangential}} = 0 \tag{8}$$

3.2.3. Heat transfer equations

In order to reduce the complexity of simulation heat transfer within the frozen congee rice during microwave processing, the assumptions were following:

1. The heat transfer was not considered in the air and PP (polypropylene) tray due to negligible dielectric loss factor.
2. The food compartments were considered as homogeneous and isotropic material.
3. The mass transport and momentum transfer of moisture did not consider.

After calculated the microwave dissipated power term, Q_{abs} by Equation (7). The Fourier heat transfer equation plus a generation term, coupled with the quasi-static electromagnetic field equation was given by:

$$\rho C_p \frac{\partial T}{\partial t} = \nabla(k \cdot \nabla T) + Q_{\text{abs}} \tag{9}$$

where ρ was the sample density [kg m^{-3}], C_p was the specific heat capacity at constant pressure [kJ $(\text{kg}^{\circ}\text{C})^{-1}$], k was the thermal conductivity [$\text{W}(\text{m}^{\circ}\text{C})^{-1}$], and T was the temperature [°C] at time t.

The surface of the food exchanged heat with the surrounding air by convection mode expressed as:

$$-n \cdot k\nabla T = h(T - T_{\text{air}}) \tag{10}$$

where n represented the normal direction to the food surface, h was the surface convective heat transfer coefficient [$\text{W}(\text{m}^{\circ}\text{C})^{-1}$], T_{air} was the air temperature [°C] and T was the transient temperature [°C].

In this work, heat loss to the air from the load was approximated by assuming convective heat transfer coefficient of value 10 $\text{W}(\text{m}^{\circ}\text{C})^{-1}$. This value was valid because this work turned off the air going inside the cavity. The air temperature was

Table 1. Summary of initial conditions and material properties applied in the model.

Parameter	Domains	Value	Source
Initial temperature, T [°C]	Air	25	–
	Ready frozen congee	−18	–
Heat transfer coefficient, h [$Wm^{-2}°C^{-1}$]	Sample-air	10	–
Electromagnetic properties			
Microwave frequency [GHz]	Cavity	2.45	–
Dielectric properties	Air	1	–
Dielectric constant, ε' [−]	Ready frozen congee (0 to 80 °C)	$-29.9 \times 10^2 T^{-2} + 3.133T^{-1} + 22.41$	Klinbun and Rattanadecho (2017)
Dielectric loss factor, ε'' [−]		$-12.1 \times 10^2 T^{-2} + 1.626T^{-1} + 2.196$	
Thermal properties			
Density, ρ[kg m^{-3}]	Ready frozen congee	989.19 (−18 to 0 °C) 1038.50 (0 to 80 °C)	Klinbun and Rattanadecho (2017)
Specific heat capacity, C_p[kJ $kg^{-1}°C^{-1}$]		2.28 (−18 to 0 °C) 3.87 (0 to 80 °C)	
Thermal conductivity, k[W $m^{-1}°C^{-1}$]		1.81 (−18 to 0 °C) 0.58 (0 to 80 °C)	

set 25° C and sample was assumed at uniform initial temperature, T_0, of −18° C. Additional input parameters used in the simulation were summarized in Table 1.

3.2.4. Simulation procedure

The numerical procedures to determine the electromagnetic field distribution and temperature profile of the frozen congee rice were started: (1) to solve Maxwell's equations to get power dissipation term inside the sample, (2) to solve heat transfer equation to predict transient temperature in sample. In this study, the commercial software based on the finite element method (FEM), COMSOL Multiphysics (version 4.3a) was used for solving the coupled electromagnetic and heat transfer model. As with other commercial software, there were four main steps to find the solution. Step 1: to build a three-dimensional model from the frozen congee structure and microwave system. From step 1, to get two models as called 'EM model' and 'HT model'. Step 2: to estimate the electric field distribution within the microwave oven and to obtain the internal heat generations for temperature analysis in 'HT model'. Step 3: to couple 'EM model' and 'HT model' were carried out continuously until the desired heating time was reached. The estimated results could show the change in figure and animation directly in step 4. A Dell Precision T7500 workstation with an operating memory of 72 GB RAM running on two quad-core Intel Xeon X5570 2.93 GHz frequency processor used to perform the simulations.

In this study, various meshing schemes for different domains were implemented to ensure the simulation results were independent of meshing. Air domain was assigned with free tetrahedral elements; frozen sample was assigned with quadrilateral element. From the work of Liu et al. (2013), the best finite element mesh size in dielectric materials for faster computation time and good accuracy temperature prediction at 2.45 GHz was shown as

Table 2. Comparison of surface temperature measurement and statistical analysis.

	Temperature (°C)			
Position	Rep1	Rep2	Rep3	SD
A0	93.43	98.05	88.82	4.62
A1	89.89	92.87	98.09	4.15
A2	90.67	94.65	90.45	2.36
A3	91.51	92.42	87.44	2.65
A4	89.60	92.1	88.73	1.75

$$h_{es} = \frac{\lambda}{6\sqrt{\varepsilon'}} \tag{11}$$

where $\lambda = 12.22$ cm. The minimum element size was bigger than 0.02 in order to faster convergence in COMSOL Multiphysics (4.3a). The time step should be neither too big nor too small. If the time step was too big, the divergence of the temperature fields would occur. The time step was too small, the convergence of the temperature field would be reached but at the expense of longer simulation time. Thus, the optimize time was performed for the total heating time 300 s with time steps ranging from 1 to 300 s. In this work, time step of 1 s was used in the simulation.

4. Results and discussion

4.1. Validation for microwave heating of frozen models

The temperature profiles after 300 s of heating were compared between the simulated and experiment as shown in Figure 3(a,b). The model parameters used in this study were shown in Table 1. In this model, it was shown without mass transfer physics.

Figure 3 shows that the contour of temperature from simulation and experimental on the right side and left side, respectively. The experiment did three replicates and thermal infrared camera used to capture the thermal figures at the surface of the sample. Table 2 shows a comparison of surface temperature measurement and statistical analysis. It was found that the SD was not exceeding 5 °C. From Figure 3, it was shown the location of the hot and cold pattern in the frozen congee rice. The simulated spatial temperature profile thermal patterns were in agreement with the experimental thermal images. It was evident that simulated temperature profiles were higher than the experimental profiles. The simulated temperature contours of thawing congee, a major portion remained about 75 °C after 300 s of microwave heating and the high temperature occurred at the centre and the side around 130 °C. The experimental was approximately 7 °C lower in temperature than the simulated thawing congee frozen. This was because of neglecting evaporation term in the simulation model. The evaporation of liquid water from the surface took away a large amount of thermal energy, so the temperature remained constant during phase change. Therefore, it was necessary to incorporate mass transfer physics to the model longer duration microwave heating process. In addition, it was shown the significant effect of non-uniform heating in a domestic microwave oven. However, a simulated model can help in optimizing the product layout, thickness, and modifying the properties of the food system.

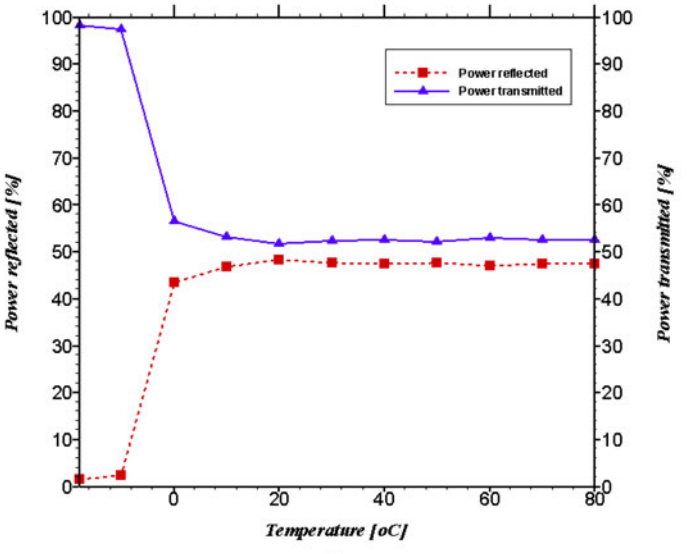

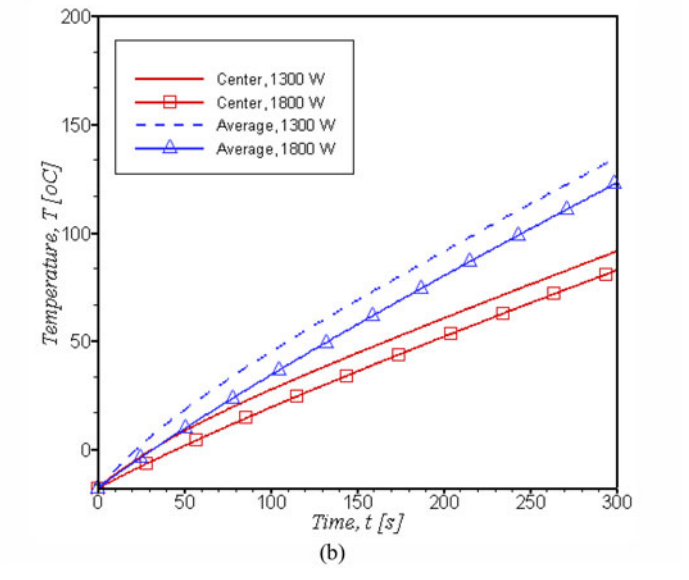

Figure 4. (a) Total percentage of microwave power reflection and transmission during microwave heating of frozen congee with minced pork. (b) Effect of microwave power intensities on heating congee with minced pork at 2.45 GHz (300 s).

The calculated temperature was compared with the average measured temperature at each point at 2.45 GHz. The results were shown in the root-mean-square error (RMSE) value. The equation was following (Pitchai et al. 2014):

$$RMSE = \sqrt{\frac{1}{N}\sum_{i=1}^{N}(T_s - T_e)^2} \tag{12}$$

where T_s and T_e were the simulated and experimental transient point temperatures, respectively. N was the total number of time steps recorded during the heating. The RMSE value was the deviation between the simulated and experimental temperatures at different points over time.

Figure 2 displayed the temperature point of heating comparison between simulation and experimental during 300 s. Figure 2 was shown that the good prediction results. The RMSE value ranged from 6.14 to 12.88 °C. The transient point temperature profiles of model were generally higher than the experiment for all three locations (L1, L3, L5). The relative error at location 3 (RMSE = 6.14 °C) was much smaller in magnitude than at locations 1 and 5. The smaller magnitudes of temperature rise at those locations because they did not absorb as much microwave energy. The hot spot was the critical point to concern in microwave heating in terms of food safety because it may because of packaging melting. Therefore, the accurate prediction of the hot spot in the model showed the promise of the simplified model.

4.2. Percentage of microwave power

Figure 4(a) plotted the microwave power (P_r, P_t) over the heating time. The equations used for calculation power reflected, P_r, and power transmitted, P_t, values given by Buffler (1993) were respectively defined as:

$$P_r = \left(\frac{\sqrt{\varepsilon'}-1}{\sqrt{\varepsilon'}+1}\right)^2 \tag{13}$$

$$P_t = 1 - P_r \tag{14}$$

From Figure 4(a), P_t was higher than P_r over the temperature range of −18 to 0 °C. The P_t and P_r values were no significant differences during 0–80 °C. The power absorption was related to the dielectric properties of frozen food during the microwave heating process. The high dielectric constant has higher power reflected. Starting at the heating at −10 °C, the dielectric properties of frozen congee were very low as 2.5-i (Klinbun and Rattanadecho 2017). Then, at 0 °C, the dielectric properties of the thawed congee increased considerably was 22.41–2.196-i. From the work of Zhang and Datta (2003), the frozen food absorbed less microwave energy than defrosted food because water molecules in the frozen food were in the crystallized state. However, the frozen congee also absorbed a relatively large amount of microwave energy because of high penetration depth (around 80% of thawed product). The microwave power absorption inside the frozen food increased slightly after the thawing state.

4.3. Effect of microwave power densities on temporal and electromagnetic characterization

To understand the effect of microwave power input on heating of frozen congee, the simulated temperature profile within frozen congee was shown in Figure 4. The

comparison between the microwave power of 1300 and 1800 W investigated in this work. The higher power resulted in greater power dissipation. The dissipation was a factor that determined the effective penetration of the microwave. From Figure 4, the relation between temperature and microwave power was linearly increased. It also found larger differences in tempering time of samples initially at $-18\,^{\circ}C$ after 60 s of microwave heating. The temperature was lower than average temperature because the cold spot occurred at the centre of frozen congee. The power absorption was explained from the previous equations. In addition, the heating time decreases by 12.6% or about 29 s during the process as a result of saving the energy input. The highest power level of 1800 W resulted in thermal runaway. Following the previous work lowering the effective electric field or the voltage across the sample thickness to avoid dielectric breakdown (arcing) during microwave heating that occurred if the electric field strength across the sample was too high. A model including phase change, conduction, and convection heat transfer was the comprehensive model to help in evaluating the power absorbed during the microwave heating process of frozen congee with minced pork.

4.4. Effect of aspect ratio on temporal and electromagnetic characterization

The effect of frozen congee size on uniformity and heating rate was shown in Figure 5(a,b), respectively. The non-uniformity of temperatures contour seen in Figure 5(a), which displayed the temperature over a midsection. In Figure 5(a), they have shown the common pattern that the high temperatures for each size were near middle while the highest temperatures were at the edge. In Figure 5(b), comparison of temperatures at centre and average for various sizes, the lowest temperature was the height of 4 mm and radius of 6 mm while the height of 6 mm and radius of 4 mm congee was the most efficient in energy absorption over the heating process. This was because of the significant penetration depth effect. In addition, the time when non-uniformity was highest extends as size increased. A longer heating period was needed before the centre starts to change the temperature in a larger size and leads to greater differences between the surface and certain regions. However, Figure 5(a) was shown 5 cm in radius and 5 cm in height of frozen congee to be typically the most uniform temperature distribution over the entire heating duration.

5. Conclusions

This study showed microwave heating of frozen congee with minced pork validation between mathematical models without mass transfer physics and experiment. Whether there was little difference in overall heating rate and uniformity. It was found that the predicted model was a higher temperature than experimental food matrix results. Thus, it was necessary to include mass transfer terms in microwave heating of Thai frozen foods model, especially when they were heated for a longer duration. In the frozen temperature range, both dielectric and thermal properties rapidly changed with increasing temperature. And then, those properties slightly varied with the temperature at thawed temperature range. The heating uniformity and thawing time depended on

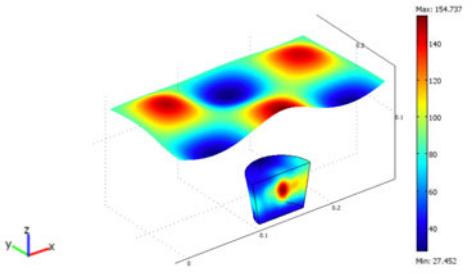

R04H06 – radius 4 cm and height 6 cm

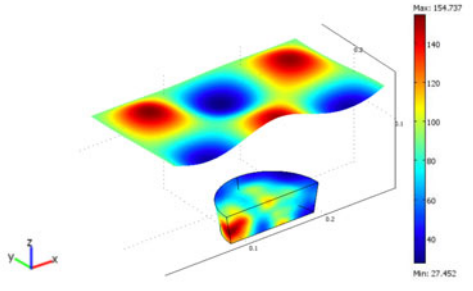

R05H05 – radius 5 cm and height 5 cm

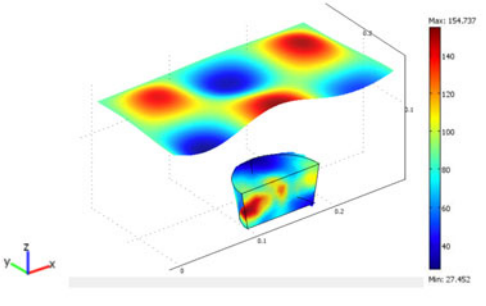

R05H05 – radius 5 cm and height 5 cm

(a)

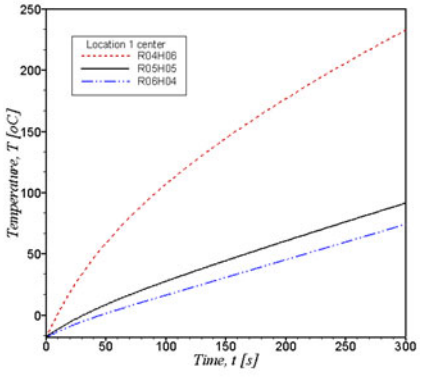

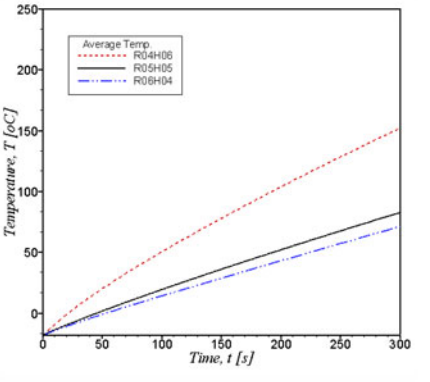

(b)

Figure 5. The electric field distribution and temperature profile of frozen congee with various aspect ratios at 300 s (P = 1300 W, f = 2.45 GHz).

power density and size of the sample. Overall, the model has been a powerful tool and effective way of predicting microwave heating rate and the uniformity.

5.1. Practical applications

The results were to be basic information for food product developers. They would understand the effects of power input, aspect ratio and materials properties (dielectric and thermal properties) on temperature distribution inside the frozen food during

the microwave heating process. In addition, these results could fill the gap in knowledge of thaw frozen food by the microwave oven.

Disclosure statement

No potential conflict of interest was reported by the authors.

Funding

The authors gratefully acknowledge the financial support provided by the Higher Education Research Promotion and National Research University Project of Thailand, Office of the Higher Education Commission and Thailand Research Fund under contract nos. RTA5980009 and TRG5780223.

Notes on contributors

Waraporn Klinbun, PhD Dr. Waraporn obtained her doctor's degree from the Thammasat University, Thailand. She has been authored and coauthored over 10 publications including ASME journal of Heat Transfer, International Journal of Heat and Mass Transfer, International Journal of food properties, Drying Technology An International Journal, Applied Mathematical Modelling. She was researcher in Professor Phadungsak research Team. Her current research focuses on using microwave technology in food processing.

Professor Dr. Phadungsak Rattanadecho is particularly interested interdisciplinary research, especially in-depth research works with academic merits, and has produced more than 80 numerous published research papers in international academic journals. His works have been cited in international research database more than 900 times. He has also been a reviewer for more than 50 international academic journals, and supervises 14 Ph.D scholarship students. In addition, his works have won more than 80 national and international awards, and more than 12 of his research works have been patented. Currently, Prof. Dr. Phadungsak is the TRF Senior Research Scholar and a head of Center of Excellence in Electromagnetic Energy Utilization in Engineering (CEEE) the Department of Mechanical Engineering, the Faculty of Engineering, Thammasat University. He obtained his Bachelor's Degree in Mechanical Engineering from King Mongkut's University of Technology Thonburi, his Master's Degree and Ph.D. in the same field, with the Japanese Government Scholarship (Monbusho), from Chulalongkorn University and Nagaoka University of Technology respectively, and Post Doctoral Fellow in Statistical Modelling Computation from University of Minnesota, Twin cities, USA. Prof. Dr. Phadungsak is an expert Modern Computational Techniques, research on heat and mass transferring in electromagnetic waves, and biomechanics. His research has now been used as a platform on which new commercially variable inventions will be made and eventually patented. Environmental minded, he studied new environmentally-friendly alternative energy. One of his outstanding pieces of research is on Computational Heat and Mass Transfer in Porous Media, Computational Heat and Mass Transfer in Phase Change Materials, Computational Heat and Fluid Flow in Human Body, Biomechanics and Microwave Heating Technology.

References

Basak T, Ayappa KG. 1997. Analysis of microwave thawing of slabs with effective heat capacity method. AIChE J. 43(7):1662–1674.

Basak T, Ayappa KG. 2002. Role of length scales on microwave thawing dynamics in 2D cylinders. Int J Heat Mass Transfer. 45(23):4543–4559.

Basak T. 2003. Analysis of resonances during microwave thawing of slabs. Int J Heat Mass Transfer. 46(22):279–4301.
Boillereaux L, Curet S, Hamoud-Agha MM, Simonin H. 2013. Model-based settings of a conveyorized microwave oven for minced beef simultaneous cooking and pasteurization. IFAC Proc. 46(31):193–198.
Buffler CR. 1993. Microwave cooking and processing: engineering fundamentals for the food scientist. Van Nostrand Reinhold, New York: Springer.
Campañone L, Paola CA, Mascheroni R. 2011. Modeling and simulation of microwave heating of foods under different process schedules. Food Bioprocess Technol. 5:738–749.
Chen F, Warning AD, Datta AK, Chen X. 2016. Thawing in a microwave cavity: comprehensive understanding of inverter and cycled heating. J Food Eng. 180:87–100.
Chen J, Pitchai K, Birla S, Gonzalez R, Jones D, Subbiah J. 2013. Temperature-dependent dielectric and thermal properties of whey protein gel and mashed potato. Trans ASABE. 56(6), 1457–1467.
Chen J, Pitchai K, Birla S, Jones D, Negahban M, Subbiah J. 2016. Modeling heat and mass transport during microwave heating of frozen food rotating on a turntable. Food Bioprod Process. 99:116–127.
Chen J, Pitchai K, Birla S, Negahban M, Jones D, Subbiah J. 2014. Heat and mass transport during microwave heating of mashed potato in domestic oven—model development, validation, and sensitivity analysis. J Food Sci. 79(10):E1991–E2004.
Choi Y-H. 1986. Effects of temperature and composition on the thermal conductivity and thermal diffusivity of some food components. In: Le Maguer M, Jelen P, editors. Food engineering and process applications. London: Elsevier Applied Science Publishers; p. 93–101.
Delgado AE, Sun D-W. 2003. One-dimensional finite difference modelling of heat and mass transfer during thawing of cooked cured meat. J Food Eng. 57(4):383–389.
Erchiqui F, Annasabi Z, Souli M, Slaoui-Hasnaoui F. 2015. 3D numerical analysis of the thermal effect and dielectric anisotropy on thawing frozen wood using microwave energy. Int J Therm Sci. 89:58–78.
Fouad E. 2013. Analysis of power formulations for the thawing of frozen wood using microwave energy. Chem Eng Sci. 98:317–330.
Geedipalli SSR, Rakesh V, Datta AK. 2007. Modeling the heating uniformity contributed by a rotating turntable in microwave ovens. J Food Eng. 82(3):359–368.
Guttman FM, Bosisio RG, Bolongo D, Segal N, Borzone J. 1980. Microwave illumination for thawing frozen canine kidneys: (A) assessment of two ovens by direct measurement and thermography. (B) The use of effective dielectric temperature to monitor change during microwave thawing. Cryobiology. 17(5):465–472.
He X, Liu R, Tatsumi E, Nirasawa S, Liu H. 2014. Factors affecting the thawing characteristics and energy consumption of frozen pork tenderloin meat using high-voltage electrostatic field. Innov Food Sci Emerg Technol. 22:110–115.
Hoke K, Houska M, Kyhos K, Landfeld A. 2002. Use of a computer program for parameter sensitivity studies during thawing of foods. J Food Eng. 52(3):219–225.
Jiao Y, Tang J, Wang S, Koral T. 2014. Influence of dielectric properties on the heating rate in free-running oscillator radio frequency systems. J. Food Eng. 120:197–203.
Klinbun W, Rattanadecho P. 2017. An investigation of the dielectric and thermal properties of frozen foods over a temperature from –18 to 80 °C. Int J Food Prop. 20(2):455–464.
Koray Palazoğlu T, Miran W. 2017. Experimental comparison of microwave and radio frequency tempering of frozen block of shrimp. Innov Food Sci Emerg Technol. 41:292–300.
Lee MZC, Marchant TR. 2004. Microwave thawing of cylinders. Appl Math Model. 28(8): 711–733.
Liu L, Llave Y, Jin Y, Zheng D, Fukuoka M, Sakai N. 2017. Electrical conductivity and ohmic thawing of frozen tuna at high frequencies. J Food Eng. 197:68–77.
Liu S, Fukuoka M, Sakai N. 2013. A finite element model for simulating temperature distributions in rotating food during microwave heating. J Food Eng. 115(1):49–62.

Llave Y, Liu S, Fukuoka M, Sakai N. 2015. Computer simulation of radiofrequency defrosting of frozen foods. J Food Eng. 152:32–42.

Llave Y, Mori K, Kambayashi D, Fukuoka M, Sakai N. 2016. Dielectric properties and model food application of tylose water pastes during microwave thawing and heating. J Food Eng. 178:20–30.

Meng Q, Lan J, Hong T, Zhu H. 2018. Effect of the rotating metal patch on microwave heating uniformity. J Microw Power Electromagn Energy. 52(2):94–108.

Moreno FL, Robles CM, Sarmiento Z, Ruiz Y, Pardo JM. 2013. Effect of separation and thawing mode on block freeze-concentration of coffee brews. Food Bioprod Process. 91(4): 396–402.

Murakami EG, Okos M. 1989. Measurement and prediction of thermal properties of foods. Food Prop Handb. 168:165–168.

Pitchai K, Birla SL, Subbiah J, Jones D, Thippareddi H. 2012. Coupled electromagnetic and heat transfer model for microwave heating in domestic ovens. J Food Eng. 112(1–2): 100–111.

Pitchai K, Chen J, Birla S, Gonzalez R, Jones D, Subbiah J. 2014. A microwave heat transfer model for a rotating multi-component meal in a domestic oven: development and validation. J Food Eng. 128:60–71.

Punathil L, Basak T. 2016. Microwave processing of frozen and packaged food materials: experimental. Reference Module in Food Science, Elsevier. ISBN 9780081005965. doi:10.1016/B978-0-08-100596-5.21009-3.

Rakesh V, Datta AK. 2013. Transport in deformable hygroscopic porous media during microwave puffing. AIChE J. 59(1):33–45.

Rattanadecho. P. 2004. Theoretical and experimental investigation of microwave thawing of frozen layer using a microwave oven (effects of layered configurations and layer thickness). Int J Heat Mass Transfer. 47(5):937–945.

Taher BJ, Farid MM. 2001. Cyclic microwave thawing of frozen meat: experimental and theoretical investigation. Chem Eng Process Process Intensif. 40(4):379–389.

Zhang H, Datta AK. 2003. Microwave power absorption in single- and multiple-item foods. Food Bioprod Process. 81(3):257–265.